Imaging sub-surface defects in power electronic modules using shear-force microscopy

Vijay Venkatesh
Mechanical & Aerospace Engineering
The Ohio State University
Columbus OH, United States
Email: venkatesh.38@osu.edu

Shailesh N. Joshi
Toyota Research Institute of North America
Ann Arbor MI, United States
Email: shailesh.joshi@toyota.com

Vishnu Baba Sundaresan
Mechanical & Aerospace Engineering
The Ohio State University
Columbus OH, United States Email:
sundaresan.19@osu.edu

Abstract – Recent advances in non-destructive evaluation (NDE) techniques have enhanced our understanding of failure mechanisms in power electronic systems. In this proceedings article, we demonstrate shear-force microscopy as a technique to map sub-surface voids in an electronic Si die soldered to a thermal sink. The proposed technique utilizes two piezoelectric wafers (dither and receiver) fitted to a scanning probe to monitor structural health of a substrate. The dither imparts high-frequency ultrasonic waves to a thin film of dielectric layer above the electronic device while the receiver detects attenuated reflected waves from the semiconductor device. The depth of penetration of ultrasonic waves in the device is controlled by varying the actuation frequency and input voltage to the dither. Presence of localized damages within the device affect mechanical boundary conditions of the vibrating probe which consequently manifests as a change in slope of the shear-force approach curve over the device. A shear-force regulated constant distance point scan is performed over a 1 mm^2 area of the electronic device, and the slope of the approach curve at each point is used as a metric to trace the contour of the void between the Si die and solder layer. The contour of the damage mapped using a grid scan bears close resemblance to that reproduced using a confocal scanning acoustic microscope. We expect that this technique can be scaled up to a NDE technique in which a spatially distributed array of piezoelectric actuation elements are kept in close proximity to the microelectronic device and separated by a dielectric gel. The shear force signature between the piezoelectric actuation elements and the surface can precisely detect structural problems during testing of accelerated aging and aggressive thermal cycling of power electronic devices.

Keywords — shear-force, power electronic device, sub-surface imaging

I. Introduction

Characterization of elastic properties at the nanoscale has received considerable attention with growing advances in non-destructive evaluation techniques. Among the various modalities that have been employed to investigate elastic properties, methods such as ultrasonic force microscopy [1], atomic force acoustic microscopy (AFAM) [2], scanning near-field ultrasound holography [3] have become de-facto standards. These techniques utilize contact forces between a scanning tip (measuring a few hundreds of nanometers) and substrate to record stiffness properties of the substrate. While the interaction volume between the tip and substrate is determined by the tip size and has been used to measure stiffness properties of the substrate, the stresses generated by the scanning tip penetrate to a near-field distance within the substrate, and allow for detection of sub-surface properties [4]. This characteristic phenomena has been used to examine defects such as nanoparticles, cracks, and voids within various substrates. A brief summary of the near-field distance detected using various scanning probe techniques is summarized in *Table 1*. The near-field distance of these acoustic waves is however limited to a few hundreds of nanometers and hence, these techniques are unable to detect features that are buried deep within a substrate. In this proceedings article, we demonstrate shear-force microscopy as a method to examine sub-surface defects in medium to hard substrates and use this technique to detect sub-surface voids in a multilayer Si die soldered to a copper heat sink.

Table 1: Near-field distance of various scanning probe techniques described in literature

Technique	Near-field distance	Defect detected	Ref.
Atomic force acoustic microscopy	200 nm	Al nanostructures	[2]
Ultrasonic force microscopy	2 nm	Graphite flakes embedded in GaAs substrate	[5]
Heterodyne microscopy	82 nm	Au nanoparticles	[6]
Scanning near-field ultrasound holography	500 nm	Au nanoparticles	[7]
Shear-force microscopy (this paper)	180 µm	Void between the Si die and solder interface	-

Shear-force microscopy

A schematic representation of a shear-force microscope hardware is depicted in *Fig. 1*. This technique utilizes a scanning probe fitted with two piezoelectric wafers (dither and receiver) to measure the structural health of a substrate. The scanning probe is oscillated at a frequency f_d using the dither to generate ultrasonic waves that propagate within the

Financial support was provided by the member organizations of the Smart Vehicle Concepts Center, a Phase III National Science Foundation Industry-University Cooperative Research Center (www.SmartVehicleCenter.org) under grant NSF IIP 1738723.

2377-5726/20/$31.00 ©2020 IEEE
DOI 10.1109/ECTC32862.2020.00221

substrate. The near-field distance of these ultrasonic waves depend on oscillation amplitude of the scanning probe. The oscillation amplitude of the probe is controlled by varying the input voltage to the dither. Presence of an isolated damage within the substrate results in a coupled interaction between the probe and substrate within a localized volume, thus affecting the mechanical boundary conditions of the vibrating probe. This resulting shift in mechanical boundary condition influences oscillatory dynamics of the scanning probe and alters electrical voltage response across the receiver while the probe approaches the substrate at a constant velocity [8]. The change in electrical voltage across the receiver (also known as 'shear-force amplitude') can be plotted as a function of the distance of the scanning probe from a substrate and is commonly referred to as an 'approach curve' in literature [9]. The variations in the slope of the approach curve above a damaged location and healthy site is used as a metric in this paper to reproduce the contour of the void between the solder layer and the Si die as outlined in *Section II-C*.

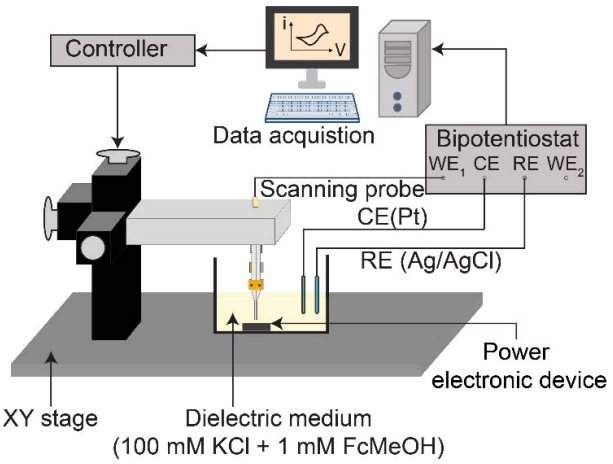

Figure 1: Schematic depiction of a shear-force microscope. The dither and receiver are mounted on the scanning probe to detect sub-surface features in a power electronic device.

Organization of this paper

The objective of the research presented in this paper is to characterize sub-surface defects in a Si die soldered to a thermal heat sink using shear-force microscopy. Towards this goal, we examine effects of (i) excitation frequencies (f_d) of the scanning probe, and (ii) dither actuation amplitude on the near-field distance of ultrasonic waves using a shear-force microscope hardware. Tuning the actuation frequency and dither actuation amplitude allows for investigation of voids between the solder layer and Si die below the surface of the device. The contour of the void reproduced using this technique is compared to a reference image mapped using a confocal scanning acoustic microscope (C-SAM). Finally, sub-surface voids within the device are modeled using a surface-impedance method and a mathematical interpretation of experimental data is presented. Our results indicate that shear-force microscopy can be extended to image different interfacial defects such as delamination and debonding at a desired subsurface interface by tailoring the actuation frequency of the scanning probe and dither actuation amplitude.

II. Materials and Methods

A. Fabrication of the scanning probe

The scanning probe used in this experiment is an ultra-microelectrode which was fabricated using a systematic procedure described elsewhere [10]. Briefly, quartz capillaries (L.: 10 cm, O.D.: 1.0 mm, I.D.: 0.5 mm, Sutter Instrument, USA) were cleaned using nitric acid solution (ACS reagent, 70%, Sigma-Aldrich) and rinsed with deionized water (Type 1, Millipore). A Pt wire (25 µm dia, Goodfellow Inc.), was inserted inside the capillary to test the electrochemical activity of the Si die. The capillaries were pulled using a P-2000 laser-based pipette puller to form an hourglass shape and reinforced with a borosilicate capillary to provide robustness. The glass capillary was polished in a MHK 1A microelectrode polisher (HEKA Elektronik Dr. Schulze GmBH) until the diameter at the tip of the capillary measured 30 µm. The Pt at the tip of the UME measured approximately 960 nm in diameter. It should be mentioned that the UMEs were fabricated with Pt to test electrochemical conductivity of the Si die. The Pt core does not affect shear-force characteristics of the scanning probe as outlined elsewhere [11].

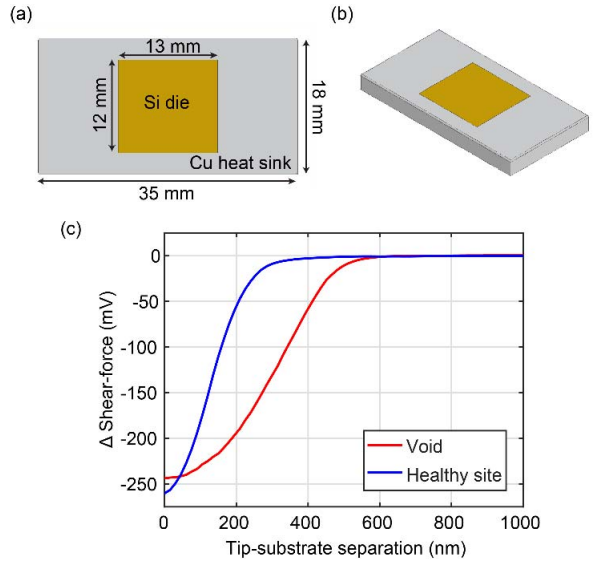

Figure 2: (a), (b) Pictorial representation of the power electronic module procured from Toyota Engineering & Manufacturing, North America, (c) Approach curve recorded over a void (defect) and healthy site. The sense length over the void is approximately 600 nm while that over a healthy site is 400 nm.

B. Experimental setup

Power electronic devices were procured from Toyota Engineering & Manufacturing, North America. A schematic

representation of the device is shown in *Fig. 2(a)-(b)*. The device consists of a 13 mm × 12 mm Si die (400 µm thickness) soldered to a 35 mm × 18 mm copper base plate (3 mm thickness). The Si die was sputtered with 300 nm Au to obtain a surface with uniform electrochemical conductivity.

The power electronic device was immersed in a dielectric medium (1 mM ferrocene methanol (FcMeOH) mixed 100 mM potassium chloride (KCl)) to characterize electrochemical conductivity of the Si die. Dither and receiver piezoelectric wafers were mounted on the scanning probe at a perpendicular orientation for improved shear-force sensitivity [11]. The scanning probe was positioned over a damage site and the dither was stimulated at increasing voltage amplitudes from 50 mV – 500 mV at a frequency such that the scanning probe is 'sensitive' to the void (see Section III). The shear-force amplitude (at the receiver) was recorded as a function of the distance of the scanning probe from the Si die to generate an approach curve as shown in *Fig. 2(c)*. Subsequently, the scanning probe was retracted from the substrate and positioned above a healthy site. The approach to the surface was repeated at the sensitive frequency to generate a curve as shown in *Fig. 2(c)***.** Upon observing a change in slope of the approach curve at the sensitive frequency, an automated shear-force regulated scan algorithm was implemented across a 1 mm^2 area and the slope of the approach curve was used as a metric to trace the contour of the sub-surface defect.

III. Results and Discussion

A multi-parameter experiment was performed to understand the sensitivity of the sub-surface defect to actuation frequency and dither actuation amplitude. The actuation frequency of the probe was swept between 300 kHz – 700 kHz while the dither actuation amplitude was varied from 50 mV to 500 mV. The effects of actuation frequency and dither amplitude on the sensitivity to the defect are summarized below.

A. Effects of actuation frequency (f_d)

In our experiments, we have observed that the sub-surface void between the Si die and solder layer is sensitive only to certain frequencies. Specifically, the approach curve (shown in *Fig. 2(c)*) exhibits a slope variation between a void and healthy site only at these 'shear-force sensitive frequencies'. We hypothesize this to be a result of an interaction between the incident ultrasonic wave and the surface of the void. *Fig. 3(a)* depicts the ultrasonic wave emitted at a frequency such that the interaction between the incident wave and damage occurs at a node. In this case, the coupling between the incident wave and damage appears as a change in slope of the approach curve. However, when the interaction between the incident wave and damage occurs at an anti-node (see *Fig. 3(b)*), the coupled effects observed above the surface of the device are insufficient to detect the location of the damage. The shear-force sensitive frequencies for imaging the sub-surface defect in the power electronic device are determined through an empirical procedure as outlined in the next section.

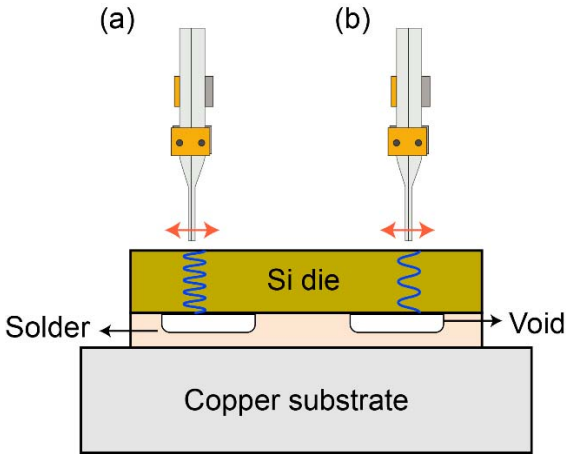

Figure 3: Schematic illustration of actuation effects on approach curve characteristics. (a) The incident ultrasonic wave interacts with the void at a node (frequency f_1) which consequently appears as a change in slope of the approach curve above the surface. (b) The interaction between the incident wave and void occurs at an anti-node (frequency f_2) and as a consequence, the approach curve does not appear to reflect this interaction.

Determination of shear-force sensitive frequencies

The shear-force sensitive frequencies for imaging sub-surface defects depends on – (a) geometry of the scanning probe, (b) relative orientation between the dither and receiver, (c) distance between the dither and receiver, (d) dither actuation amplitude, and (e) stiffness of the defect. The shear-force sensitive frequencies of the scanning probe used in this experimental study (30 µm glass tip diameter, 90° dither-to-receiver orientation and 5 mm dither-to-receiver distance) were obtained by examining the shear-force response of the scanning probe when located in the vicinity of a damaged site to that recorded on a healthy site.

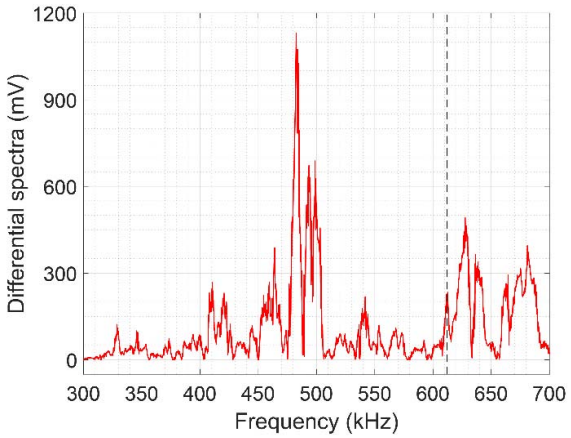

Figure 4: Differential shear-force spectra between a void and healthy site. The sensitive frequencies for sub-surface imaging are selected based on the differential spectra. The chosen sensitive frequency (f = 611.1 kHz) is shown as a dotted trace. The dither actuation amplitude was 250 mV.

Fig. 4 depicts the differential amplitude spectra between the two locations recorded at the receiver when the actuation amplitude at the dither was kept constant at 250 mV. The frequencies at which a peak is obtained are used to calibrate the approach curve above a healthy site and a damaged location. It should be mentioned that a sensitive peak in the differential spectra does not guarantee a difference in approach curve characteristics (between a void and healthy location) at the corresponding frequency, but merely isolates the possibilities of identifying sensitive frequencies from a wide range of data. For instance, we observed that the approach curve characteristics over a void and healthy site were similar at 464 kHz but exhibited a slope difference at 611.1 kHz as shown in *Fig. 4*.

B. *Effects of dither actutation amplitude*

The effects of dither actuation amplitude on sensitivity to a sub-surface defect is summarized in *Fig. 5*. Increasing dither actuation amplitude results in a higher oscillation amplitude of the scanning probe. Consequently, the near-field distance of ultrasonic waves within the substrate increases. The optimum dither actuation amplitude for achieving a near-field distance of 180 µm (with a 30 µm glass tip diameter probe) was found to be 250 mV.

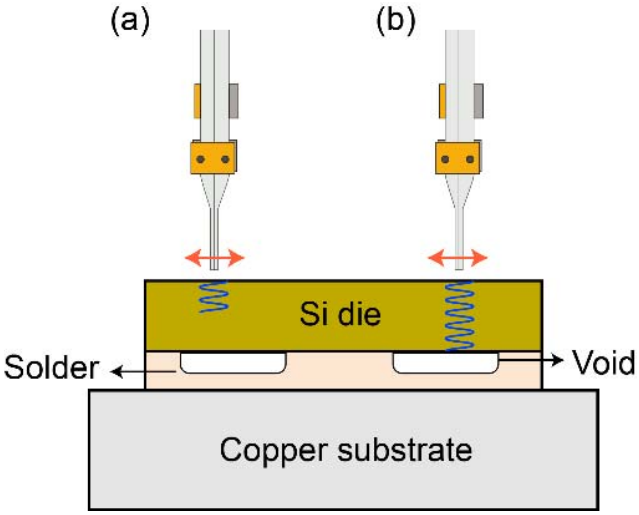

Figure 5: Effects of dither actuation amplitude on near-field distance in power electronic devices using shear-force microscopy. In (a), the near-field distance is far less than the actual defect depth due to lower actuation amplitudes (<100 mV). Increasing dither actuation amplitude to 250 mV in (b) leads to a higher penetration depth and defect sensitivity.

C. *Void description and mapping*

The optimum experimental conditions for detecting a sub-surface void between the solder layer and Si die are described in *Table 2*. These parameters were used to map the contour of a void using a shear-force regulated constant-distance point scan in the shear-force microscope hardware. A 1 mm × 1 mm area encompassing both defective spots and healthy sites were mapped using this technique. The scanning probe approached the Si die until the shear-force measured at the receiver decreased by 100 mV. The slope of the approach curve was recorded as a metric once this threshold in shear-force was met, and the scanning probe was retracted by approximately 20 µm. It is important to note that the retraction distance from the Si die was set to this value to account for the tilt in the surface of the device across the scan length in both *x* and *y* directions. The scanning probe was then translated in the *(x,y)* plane to the next location and the approach to the substrate was repeated at this pixel. An image consisting of 96 pixels/mm^2 was constructed by using the slope of the approach curve as a metric. *Fig. 6(a)* depicts the approach curves recorded over the Si die over an array of grid points encompassing the void and healthy site. It is noticed that the slope of the approach curves over the void is lesser than the value recorded over a healthy site. This is attributed to lower localized stiffness of the void-filled region underneath the Si die. The contour of the sub-surface void mapped using the slope of the approach curve as a metric is shown in *Fig. 6(b)*. It is observed that the contour bears a close resemblance to the C-SAM image of the void (see *Fig. 6(c)*).

Table 2: Optimum experimental conditions for detecting sub-surface defects in power electronic devices

Glass diameter	30 µm
Pt diameter	960 nm
Actuation frequency	611.1 kHz
Dither actuation amplitude	250 mV
Dither-to-receiver orientation	90°
Dither-to-receiver spacing	5 mm

D. *Analytical interpretation*

In this section, a mathematical interpretation for mapping sub-surface defects using shear-force microscopy is presented. The mathematical approach presented is based on a surface-impedance algorithm developed by Sarioglu and co-workers [12]. The sub-surface voids between the Si die and thermal heatsink can be modeled using the surface impedance based stiffness calculation algorithm. Assuming that the scanning probe applies shear stresses over the localized diffusion shell, the interaction volume between the probe and the substrate acts as an ultrasonic radiator with a symmetric stress distribution. The mechanical radiation impedance can be computed using Equation (1) –

$$Z(\omega) = -\int_0^\infty \left|T_{yz}(k_r)\right|^2 k_r dk_r \Big/ \int_0^\infty T_{yz}^*(k_r) V_y(k_r) k_r dk_r \quad (1)$$

where T_{yz} is the shear-stress, V_y is the particle velocity, and k_r is the radial wave number of the particular plane wave component radiated. The relation between the stress fields and particle velocity fields at the surface can be calculated using the surface impedance tensor **G** defined as –

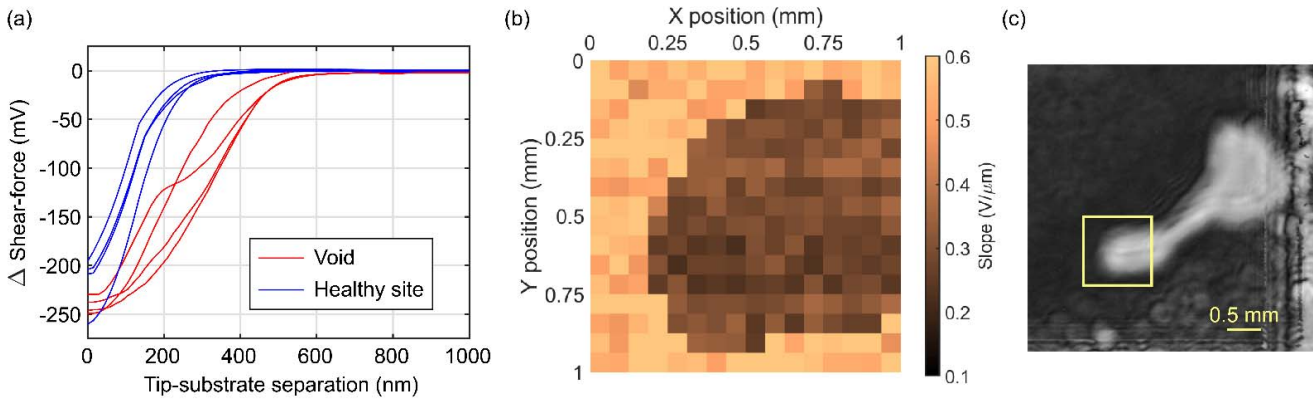

Figure 6: (a) Approach curves over a void and healthy site. (b) Shear-force microscopy image of sub-surface defects in a power electronic device. The optimum experimental conditions for imaging the device is given in Table 2. (c) C-SAM image of the void region. The region imaged in (a) is depicted alongside.

$$\mathbf{T} = \mathbf{GV} \xrightarrow{\textbf{yields}} \begin{bmatrix} T_{xz} \\ T_{yz} \\ T_{zz} \end{bmatrix} = \begin{bmatrix} G_{11} & G_{12} & G_{13} \\ G_{21} & G_{22} & G_{23} \\ G_{31} & G_{32} & G_{33} \end{bmatrix} \begin{bmatrix} V_x \\ V_y \\ V_z \end{bmatrix} \quad (2)$$

where T_{xz}, T_{yz}, and T_{zz} are the x, y, z components of the stress fields and V_x, V_y, and V_z are the particle velocities in the three directions. Assuming the scanning probe laterally vibrates above the surface only in the y-z plane, the acoustic power radiated into the substrate is determined by the y component of the particle velocity vector given by $V_y(k_r) = G_{22}^{-1}(k_r)T_{yz}(k_r)$. Since the stress distribution in the vicinity of the scanning tip is uniform, $T_{yz}(k_r) = 2\pi a J_1(ak_r)/k_r$, we obtain –

$$Z(\omega) = \frac{-\pi a^2}{2\pi a^2 \int_0^\infty \left|\left[\frac{J_1(ak_r)}{k_r}\right]\right|^2 G_{22}^{-1}(k_r) k_r dk_r} \quad (3)$$

where $J_1(.)$ is the first-order Bessel function of the first kind and G_{22}^{-1} is the element with index 2,2 in the inverse of the surface impedance matrix at the surface.

Future work would involve computation of (a) near-field distance as a function of actuation amplitude applied at the dither, and (b) localized contact stiffness of the Si die with and without a void below the surface. An automated algorithm that selects the sensitive frequency based on experimental conditions would allow for faster imaging of sub-surface defects and enable precise detection of structural problems in accelerated thermal cycling of power electronic devices.

Conclusions

In this paper, a shear microscopy hardware is used to image sub-surface defects in a Si die soldered to a thermal heat sink. A multi-parameter experiment was performed to understand the sensitivity of the void (between the Si chip and solder interface) to experimental variables such as dither actuation amplitude, actuation frequency and glass diameter of the scanning tip. A constant-distance point scan was performed across a 1 mm^2 area encompassing the void and sub-surface features were detected using the slope of the shear-force based approach curve as a metric. The contour of the void was compared to a C-SAM image of the device and our results revealed a close resemblance between the two images. An analytical interpretation of near-field distance in the hardware was further formulated. Based on the results presented in this paper, we anticipate shear-force microscopy technique to be scaled up as a non-destructive evaluation technique for enhancing our understanding of sub-surface defects during aggressive thermal cycling of power electronic devices.

References

[1] O. V. Kolosov, M. R. Castell, C. D. Marsh, G. A. D. Briggs, T. Kamins, and R. S. Williams, "Imaging the elastic nanostructure of Ge islands by ultrasonic force microscopy," *Physical review letters,* vol. 81, no. 5, p. 1046, 1998.

[2] S. Hu, C. Su, and W. Arnold, "Imaging of subsurface structures using atomic force acoustic microscopy at GHz frequencies," *Journal of Applied Physics,* vol. 109, no. 8, p. 084324, 2011.

[3] G. Shekhawat and V. Dravid, "Seeing the invisible: scanning near-field ultrasound holography (SNFUH) for high resolution sub-surface imaging," *Microscopy and Microanalysis,* vol. 12, no. S02, pp. 1214-1215, 2006.

[4] G. Yaralioglu, F. Degertekin, K. Crozier, and C. Quate, "Contact stiffness of layered materials for ultrasonic atomic force microscopy," *Journal of Applied Physics,* vol. 87, no. 10, pp. 7491-7496, 2000.

[5] K. Yamanaka, H. Ogiso, and O. Kolosov, "Ultrasonic force microscopy for nanometer resolution subsurface imaging," *Applied Physics Letters,* vol. 64, no. 2, pp. 178-180, 1994.

[6] G. Verbiest, T. Oosterkamp, and M. Rost, "Subsurface contrast due to friction in heterodyne force microscopy," *Nanotechnology,* vol. 28, no. 8, p. 085704, 2017.
[7] G. S. Shekhawat and V. P. Dravid, "Nanoscale imaging of buried structures via scanning near-field ultrasound holography," *Science,* vol. 310, no. 5745, pp. 89-92, 2005.
[8] R. G. Northcutt, C. Heinemann, and V. B. Sundaresan, "Dynamic mechanoelectrochemistry of polypyrrole membranes via shear-force tracking," *Physical Chemistry Chemical Physics,* vol. 18, no. 26, pp. 17366-17372, 2016.
[9] L. Danis, M. E. Snowden, U. M. Tefashe, C. N. Heinemann, and J. Mauzeroll, "Development of nano-disc electrodes for application as shear force sensitive electrochemical probes," *Electrochimica Acta,* vol. 136, pp. 121-129, 2014.
[10] V. Venugopal, V. Venkatesh, R. G. Northcutt, J. Maddox, and V. B. Sundaresan, "Nanoscale polypyrrole sensors for near-field electrochemical measurements," *Sensors and Actuators B: Chemical,* vol. 242, pp. 1193-1200, 2017.
[11] V. Venkatesh, R. Northcutt, C. Heinemann, and V. B. Sundaresan, "A structural model of ultra-microelectrodes for shear-force based scanning electrochemical microscopy," *Journal of Intelligent Material Systems and Structures,* vol. 29, no. 18, pp. 3562-3571, 2018.
[12] A. Sarioglu, A. Atalar, and F. Degertekin, "Modeling the effect of subsurface interface defects on contact stiffness for ultrasonic atomic force microscopy," *Applied physics letters,* vol. 84, no. 26, pp. 5368-5370, 2004.